DB2.1.1 Report on the compositions formulated and the results obtained in their characterisation

Index

1. Introduction

The actions contemplated in the LIFE EGGSHELLENCE project are structured in five groups of actions, being those of type "B" the Implementation actions of the project. This deliverable corresponds to Action B2 "Pre-industrial scale tests of ceramic wall tiles production with eggshell" and describes the results obtained by ITC-AICE, UA, EATOMIZADO and ADM in the formulation and characterization of wall tile compositions with bio-$CaCO_3$ at laboratory scale.

1.1. Use of bio-$CaCO_3$ in ceramic tiles

As already proved in Action B1, bio-$CaCO_3$ obtained from eggshells is comprised of crystalline calcium carbonate ($CaCO_3$, 94.5 wt%), magnesium carbonate ($MgCO_3$, 0.7 wt%) and calcium phosphate ($Ca_3(PO_4)_2$, 1.3 wt%), and 3.5% of organic matter (with C and N). Therefore, it can become an alternative source of calcium carbonate.

Ceramic tiles are thin slabs made from clays, silica, fluxes, calcium carbonate and other raw materials. They are generally used as coverings for floors, walls and facades. Wall tiles are the type of ceramic tiles used as coverings for walls.

One of the required wall tile properties is high dimensional stability. This is achieved by low firing shrinkage (less than 1%), which is accompanied by high porosity, facilitating tile installation.

High porosity allows the tile to be readily accessed by water, hydrating the amorphous and glassy phases present. This increases the size of the fired body, which can lead to tile curvature and even crazing of the glaze layer. It is therefore necessary for fired tiles to contain a large quantity of crystalline phases with a minimum presence of amorphous phases, to enable attaining low moisture expansion (below 0.1 %).

Dimensional stability, high porosity and crystalline phase formation are achieved by introducing calcium and/or magnesium carbonates in the composition in percentages varying from 10 to 15%. This is because at temperatures around 800-900°C, calcite and magnesium carbonates decompose into calcium and magnesium oxide and carbon dioxide. The calcium and magnesium oxides react with the amorphous phases stemming from clay mineral dehydroxylation to form calcium and/or magnesium aluminosilicates and silicates, which are stable on exposure to moisture.

As wall tiles are the type of ceramic tile that use larger amounts of calcium carbonate, this is the type of tile that will be used in the project to demonstrate the valorisation of the bio-$CaCO_3$. Different body compositions representative of those used at industrial scale by both the Spanish and the Portuguese ceramic clusters for the manufacturing of wall tiles have been designed and characterized at laboratory scale by ITC-AICE and EATOMIZADO (Spanish compositions) and UA and ADM (Portuguese compositions). These compositions have been prepared with commercial calcium carbonate ($CaCO_3$) and with the bio-$CaCO_3$ (totally and partially replacing the commercial material in the same percentages) resulting from the treatment in MAINCER facilities of the eggshell supplied by AGOTZAINA. It is important to note that this treatment is the same that later was implemented in the prototype installed in AGOTZAINA, and as checked in Action B1, the bio-$CaCO_3$ has similar characteristics.

In the following sections, the different compositions and the results obtained in their characterization are detailed and commented.

2. Spanish compositions developed by ITC-AICE

2.1. Initial tests

The first wall tile compositions developed by ITC-AICE were a STD composition with 15 wt% of mineral calcium carbonate (Table 1) and two compositions with the same percentages of calcium carbonate, clays and non plastic raw materials but replacing the mineral calcium carbonate by the bio-$CaCO_3$ resulting from the processing of the eggshell at pilot scale (C-CM) and by the same bio-$CaCO_3$ but washed to remove the small part of membrane still present (C-CL). Prior to the preparation of the compositions, bio-$CaCO_3$ samples were milled in order to have a similar particle size with respect to mineral calcium carbonate (Table 2) and then to be able to determine the possible influence of the organic matter without the interference of particle size.

Table 1 Wall tile compositions formulated.

Composition	C-STD	C-CM	C-CL
Mixture of clays	55	55	55
Calcium carbonate	15	-	-
Milled bio-calcium carbonate	-	15	-
Washed and milled bio-calcium carbonate	-	-	15
Mixture of non plastic raw materials	30	30	30

Table 2 Particle size of the mineral calcium carbonate and of the bio-$CaCO_3$ samples used in the manufacturing of wall tile compositions.

Sample	Calcium carbonate	Milled bio-calcium carbonate	Washed and milled bio-calcium carbonate
Reject at 40 μm (wt%)	0.8	1.7	5.8
Reject at 63 μm (wt%)	0.0	0.3	1.0

2.1.1. Experimental procedure

These compositions were milled at laboratory scale (Figure 1) and the spray-dried powders were obtained at pilot scale (Figure 2) and characterized by evaluating their behaviour in the manufacturing process:

- ✓ Dry bulk density.
- ✓ Firing behaviour: evolution of firing shrinkage and water absorption with firing temperature.
- ✓ Tendency to black core formation.
- ✓ Moisture expansion.

Figure 1. Laboratory milling of the compositions.

Figure 2. Spray-drier used for the preparation of the spray-dried powders.

For the determination of **dry bulk density and firing behaviour**, the spray-dried powders were used to form cylindrical test pieces (4 cm in diameter and about 7 mm thick) by uniaxial pressing, at standard pressing conditions for wall tiles: a moisture content of 5.5% (dry basis) and a pressure of 250 kg/cm^2. The test pieces were dried at 110ºC in an electric laboratory oven with air recirculation. They were then weighed, their diameter was measured and bulk density was determined by the mercury displacement method. After this, they were fired with a fast firing cycle and a residence time of 6 minutes at peak temperature in an electric laboratory kiln. The heating rate was 25°C/min.

After the test specimens had been fired, they were reweighed and bulk density was determined by the method indicated above. Firing shrinkage was evaluated as the difference between dry and fired specimen diameter; this parameter was defined on a dry weight basis. Water absorption was calculated by measuring the weight gain of the test pieces after being subjected to a vacuum pressure of 91 kPa for 30 minutes, then being immersed in water and subsequently left in the water at atmospheric pressure for 15 minutes.

For the determination of the **tendency to black core formation** 15x15 cm tiles were pressed at the pilot press of ITC-AICE (Figure 3) at standard thickness (7 mm) and at a higher thickness (12 mm), to magnify the black core that could appear due to the organic matter present in the bio-calcium carbonates (organic matter oxidation depends on the diffusion of oxygen through the tile: the higher the thickness of the tile, the lower the oxidation of the organic matter and therefore, the higher the black core formation). These pressed tiles were glazed and fired in a tile manufacturing company.

Moisture expansion was determined by measuring the expansion of the sample, fired at different temperatures, after being autoclaved for 5 hours with water vapour pressure of 10,2 kg/cm^2. In order to do this, prismatic test specimens (80 m long, 20 mm wide, and approximately 7 mm thick) were formed by uniaxial pressing. The test specimens were dried at 110°C to constant weight in an electric laboratory oven with recirculating air. They were then weighed, their diameter was measured, and bulk density was determined by the mercury displacement method. After this, they were fired with a fast firing cycle and 6 min. hold at peak temperature in an electric laboratory kiln. The heating rate was 25°C/min. Finally, moisture expansion (ME) was calculated from the following expression:

$$ME = \frac{l_h - l_f}{l_f} \cdot 1000$$

where:

− l_h: length of the hydrated specimen

− l_f: length of the fired specimen

Figure 3. Pilot press.

2.1.2. Results obtained

Table 3 shows the properties before firing and Figure 4 and Table 4 firing behaviour and the properties of the fired tiles of the three spray-dried powders. The most remarkable differences are the lower dry bulk density (higher porosity) of the specimens pressed with the compositions with the bio-calcium carbonates, that also leads to a lower density of the fired specimens and to a higher water absorption. Moisture expansion is also higher, which could be due to the higher porosity already commented. It is important to note that all these changes are not considerable and are associated to a complete substitution of the mineral calcium carbonate by the bio-calcium carbonates.

Table 3 Properties before firing of the spray-dried powders.

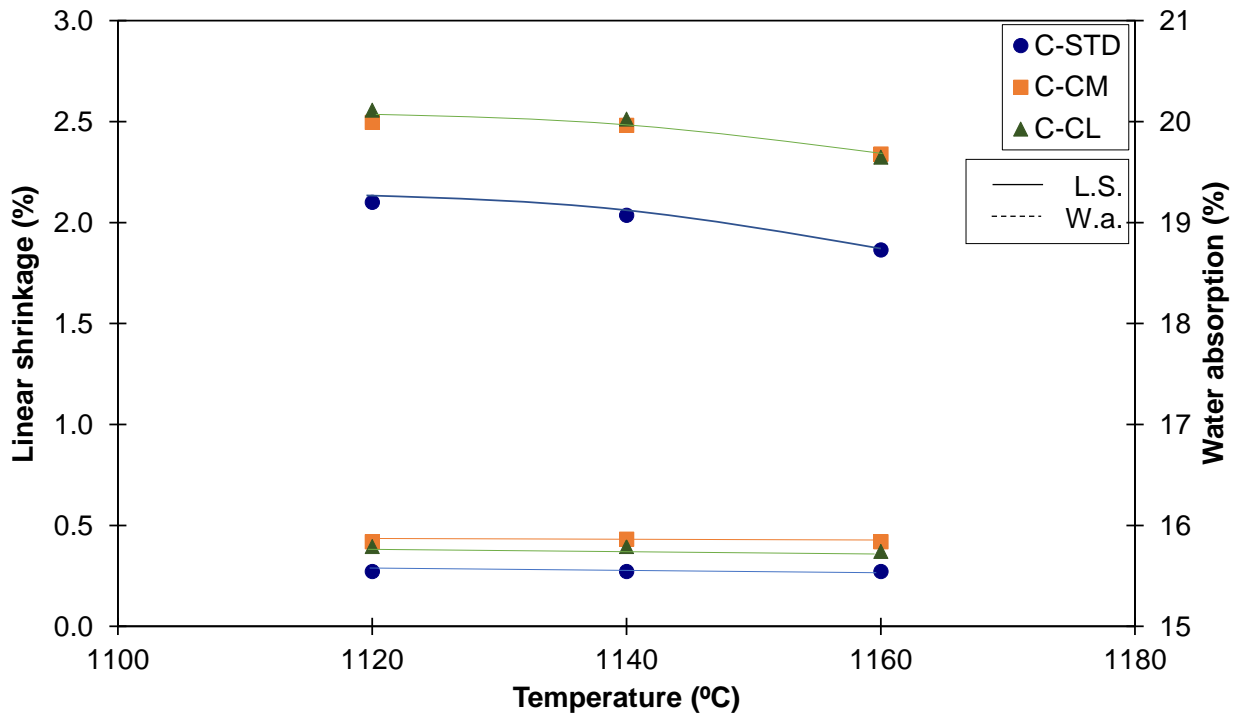| Composition	C-STD	C-CM	C-CL
Reject at 40 μm (wt%)	9.8	11.6	12.1
Reject at 63 μm (wt%)	3.7	4.9	4.6
Moisture content (%)	5.5	5.5	5.5
Pressing pressure (kg/cm^2)	250	250	250
Dry bulk density (g/cm^3)	1.948	1.913	1.917

Figure 4. Linear shrinkage and water absorption as a function of firing temperature.

Table 4 Properties of the spray-dried powders at the temperature of 1140ºC.

Composition	C-STD	C-CM	C-CL
Linear shrinkage (%)	0.27	0.43	0.40
Water absorption (%)	19.1	20.0	20.0
Loss on ignition (%)	11.04	11.25	11.10
Bulk density (g/cm^3)	1.752	1.729	1.732
Moisture expansion (‰)	0.42	0.50	0.59

The tiles obtained at pilot scale are shown in Figure 5 and in Figure 6. The thin tiles show black core (grey shadowed area) both in the case of the washed bio-calcium carbonate (somewhat lower) and in the unwashed one, while the tile with mineral calcium carbonate does not show this defect. In the tiles with high thickness, there is black core in all of them, but it is lower in the tile with mineral calcium carbonate. There are no significant differences between the two tiles with bio-calcium carbonate washed or unwashed. The black coring tendencies obtained with the two bio-calcium carbonates are not highly worrying as the bio-calcium carbonates will substitute partially and not totally the mineral calcium carbonate in wall tile compositions.
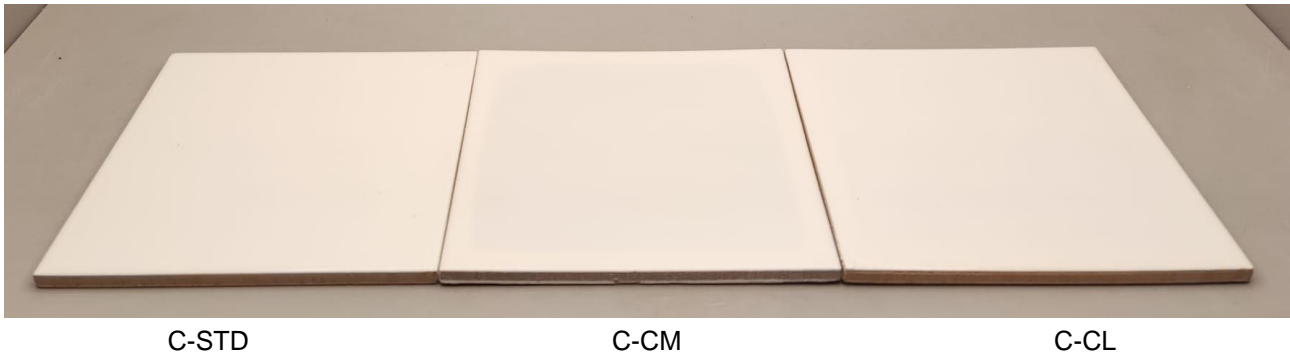
C-STD   C-CM   C-CL

Figure 5. Standard thickness tiles.

C-STD   C-CM   C-CL
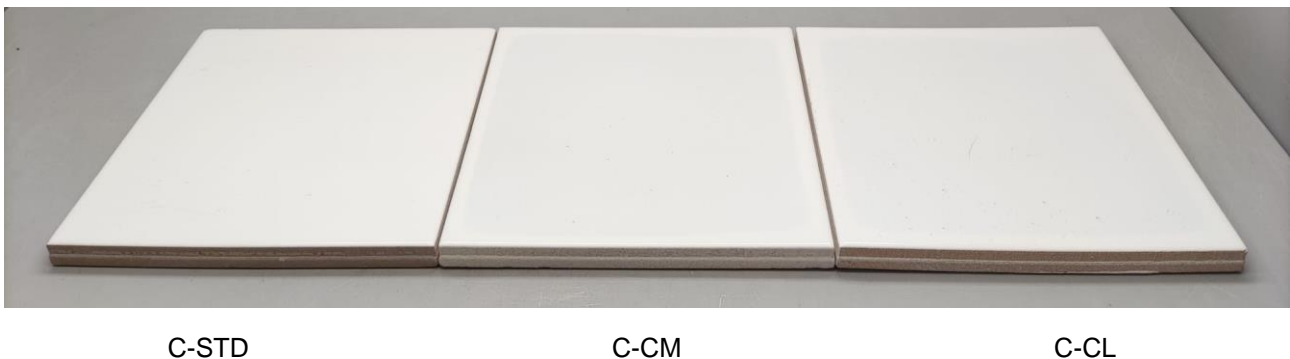
Figure 6. High thickness tiles.

These results allowed concluding in Action B1 that, as supposed, a significant part of the organic matter present in the eggshell is inside the inorganic structure.

2.2. Second tests

When discussing the previous results with the rest of the partners involved in this action, it was considered important to determine if the organic matter present in the bio-CaCO$_3$ could act as a binder. This would be very important as some compositions use organic binders to increase dry mechanical strength when large wall tiles are manufactured and the possible performance as a binder of the bio-CaCO$_3$ would be a considerable advantage with respect to the use of mineral calcium carbonate.

For this reason, a second testing was planned, with the same formulation used in the previous section. In this case only STD composition (C-STD) and the one with bio-CaCO$_3$ previously milled (but not washed, C-CM2 M) were prepared and again processed in the spray-drier.

2.2.1. Experimental procedure

The spray-dried powders were characterized by determining dry mechanical strength at constant dry bulk density (in order to avoid the interference of this parameter).

Dry mechanical strength was determined by three-point bending. For this, prismatic test pieces, 80 mm long, 20 mm wide, and about 7 mm thick, were formed by uniaxial pressing at a pressing moisture content of 5.5% (dry basis) and the pressure required to obtain a dry bulk density of 1.95 g/cm^3. The test pieces were dried in an electric laboratory oven with air recirculation at 110 °C. They were then weighed again and their bulk density was determined by the mercury displacement method.

Before the tests were performed, the test pieces were introduced in a desiccator under vacuum for the time required to reach room temperature (about 20 minutes), in order to keep their hydration to a minimum. The tests were carried out in a mechanical testing machine (Instron) at a constant deformation rate of 1 cm/min.

The three-point bending device consists of two lower supporting edges (supports), which are generally cylindrical, on which the test piece is placed, and a top support, also cylindrical, through which the load is

applied. The tensile strength of a test piece subjected to a three-point bending test is given by the following expression:

$$\sigma = \frac{3 \cdot F_{max} \cdot L}{2 \cdot b \cdot e^2}$$

where:

σ : dry mechanical strength (kg/cm^2)

F_{max} : maximum force before rupture or breaking load (kgf).

L : distance between supports (cm).

b : width of the test piece (cm).

e : thickness of the test piece (cm).

2.2.2. Results obtained

The results obtained (Table 5) show again the higher porosity of the pressed specimens with the bio-CaCO$_3$, which in this case leads to an increment of pressing pressure in order to obtain the same bulk density. On the other hand, a considerable increase of the dry mechanical strength is observed in the C-CM2 M spray-dried powder with respect to the C-STD powder, which allows concluding that, as suggested, there may be a binding characteristic in the bio-CaCO$_3$.

Table 5 Properties of the spray-dried powders.

Composition	C-STD	C-CM2 M
Moisture content (%)	5.5	5.5
Pressure (kg/cm^2)	285	350
Dry bulk density (g/cm^3)	1.946	1.946
Dry mechanical strength (kg/cm^2)	33	42

2.3. Third testing

In the previous tests, bio-CaCO$_3$ has always been used previously milled to obtain a similar particle size with respect to the mineral calcium carbonate, but the necessity for this pre-treatment had not been checked. For this reason, in this third testing, the same two compositions of the previous testing were prepared at pilot scale but with the original particle size in the case of the bio-CaCO$_3$.

2.3.1. Experimental procedure

The two compositions were prepared by wet milling (pilot scale, Figure 7) at a solids content of 67% and with a defloculant content of 0.5%. Milling time was the same for both compositions. The slurries were characterized by determining the variation of viscosity and thixotropy with time (as the possible degradation of the organic matter present in the bio-CaCO$_3$ could affect to the rheology of the suspension). The measurements were made using a GALLENKAMP viscometer with a no. 30 torsion wire using a 1.75-cm-diameter cylinder.

Figure 7. Pilot milling.

The slurries were also processed in the spray-drier as in previous tests and the spray-dried powders were characterized as previously: determining dry mechanical strength at constant dry bulk density.

2.3.2. Results obtained

The viscosity and thixotropy of the suspensions just after their milling showed higher values of both parameters in the case of the composition with bio-$CaCO_3$ (C-CM2) as it can be seen in Table 6 and in Figure 8. This increase in viscosity and thixotropy has also been observed by other partners, as it will be discussed in the following sections. In addition, Figure 8 shows that the slurry with bio-$CaCO_3$ (C-CM2) shows a considerable increase of both parameters along the time, that could be due to the degradation of organic matter previously suggested. It is important to note, however, that typically slurries are spray-dried immediately after the milling or stored few hours, so the increase observed along the time is not expected to affect industrial practice. And the higher viscosity and thixotropy of the slurry with bio-$CaCO_3$ (C-CM2) is associated with total substitution of mineral calcium carbonate and, as previously commented, pilot and industrial trials will be done with lower percentages of bio-$CaCO_3$.
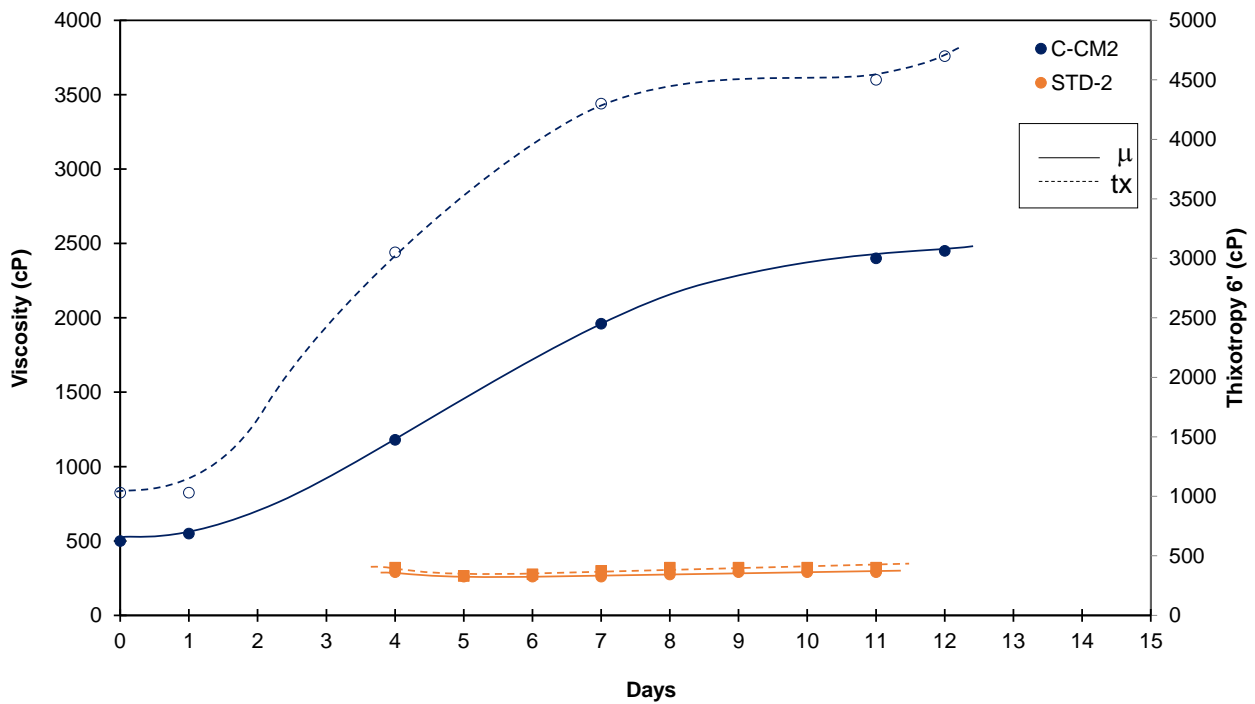
Figure 8. Variation of viscosity and thixotropy with time.

Another important result of the characterization of the slurry and of the spray-dried powder is the presence of carbonates of high particle size in the CM2 composition (both in the reject at 200 μm of the slurry and in the reject at 63 μm of the spray-dried powder) associated with the use of the bio-CaCO$_3$ without previous milling. This suggests that previous milling of the bio-CaCO$_3$ may be necessary for industrial use but it must be confirmed in industrial milling as it may change. Also, the possible influence of the carbonates of high particle size on the presence of defects in the glazed surface of the tiles has to be checked as the higher the particle size of the carbonates, the more difficult is their decomposition and this can cause pinholes in the glazed layer of the tile.

Finally, pressing behaviour and dry mechanical strength of the spray-dried powders are also detailed in Table 6, showing the previously confirmed trend of the composition with bio-CaCO$_3$, that is, requiring higher pressure and providing higher mechanical strength.

Table 6 Properties of the compositions and of the resulting spray-dried powders.

Composition	C-STD 2	C- CM2
Viscosity of the slurry (cP)	260	500
Thixotropy of the slurry (cP)	330	1030
Carbonates in the R200 μm of the slurry (%)	-	3.9
Reject at 63 μm (wt%)	3.5	3.2
Carbonates (%)	14.6	14.1
Carbonates in the R63 μm (%)	1.1	14.0
Moisture content (%)	5.5	5.5
Pressing pressure (kg/cm^2)	270	350
Dry bulk density (g/cm^3)	1.949	1.941
Dry mechanical strength (kg/cm^2)	30	37

2.4. Rheological study

The last series of testing performed by ITC-AICE prior to the pilot processing in sub-action B2, comprised a rheological study to establish optimum solids content and deflocculant and then to check if any changes with respect to the use of mineral calcium carbonate are necessary when using bio-CaCO$_3$. This is an important aspect as the reduction in solids content or the increase in deflocculant would increase the cost of the production of spray-dried powder (because of the higher energy consumption associated to an increase in the amount of water to be evaporated in the spray-drier or to the high cost of the deflocculant). Figure 9 shows the variation of viscosity with the deflocculant content of the two compositions, initially at constant solids content of 72% and in the case of the CM composition also with a lower solids content (71%). At constant solids content, the results are similar to the previous ones: an increase in viscosity in the composition with bio-CaCO$_3$, which leads to a higher demand of deflocculant. When solids content is reduced, the curve obtained is closer to that obtained with the STD composition. Optimum values from these curves are detailed in Table 7. This possible reduction in solids content and the possible increase in deflocculant will be confirmed in the pilot processing in sub-action B2.2.
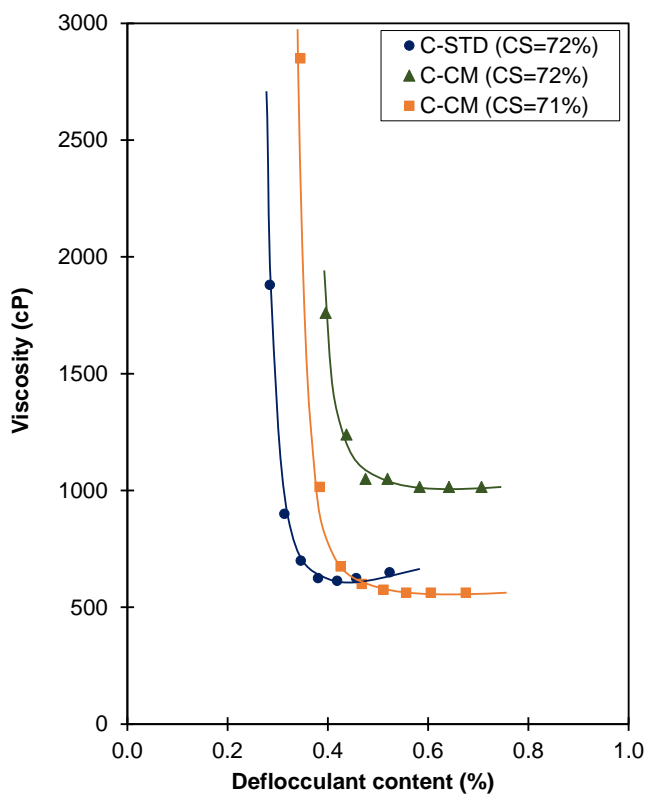

Figure 9. Variation of viscosity with deflocculant content.

Table 7 Optimum solids content and deflocculant addition.

Composition	C-STD	C-CM	
Solids content (%)	72.0	71.9	70.8
Deflocculant content (%)	0.42	0.60	0.56
Viscosity (cP)	613	1015	563

3. Spanish compositions developed by EATOMIZADO

EATOMIZADO apart from supervising the results obtained by ITC-AICE, also tested the bio-CaCO$_3$ at laboratory scale (with no previous milling) in an industrial composition substituting 100% of the mineral

calcium carbonate. Similar findings were obtained with respect to those detailed in the previous section: higher viscosity in the composition with bio-$CaCO_3$ and higher demand of deflocculant to reach minimum viscosity.

4. Portuguese compositions developed by UA

The suspensions with all the raw materials were homogenized in a turbo diluter and sieved at 425 μm. Then, to remove water from the suspension and obtain a paste with the desired humidity ($\approx$ 20 wt.%) a gypsum plate was used. The pastes were stored, at room temperature, in closed plastic bags to avoid drying until the preparation of the specimens. To evaluate the influence of the limestone substitution degree and its granulometric distribution eight formulations were prepared (Table 8). In this table, L stands for limestone, E for eggshell and D for the D50 value or median, which means that 50 vol.% of the particles have diameters equal to or smaller than this value. Moreover, the reference formulation is L100D4, 100 % of limestone with a D50 of 4 µm.

The specimens were prepared in ADM using two conformation processes: a) extrusion to obtain cylindrical specimens and b) uniaxial hydraulic pressing (RAM from MACOCER) for rectangular tiles. Before conformation, the paste was smashed to take out the air bubbles and its humidity was kept at 20 % to maintain good workability. After the conformation process, the samples were dried overnight at 105°C.

Table 8- Composition of the prepared pastes.

	Dry material composition (wt.%)					
	CaCO₃ source	Limestone		Eggshell		
	D50 (µm)	3.5	4	4	5.5	2.5
Reference	L100D3.5	100	-	-	-	-
	L100D4	-	100	-	-	-
	L75E25D4	-	75	25	-	-
	L50E50D4	-	50	50	-	-
	L25E75D4	-	25	75	-	-
	E100D4	-	-	100	-	-
	E100D5.5	-	-	-	100	-
	E100D2.5	-	-	-	-	100

The specimens were sintered in two furnaces: at the university (laboratory scale, discontinuous oven) and at a wall tiles industry (industrial scale, continuous roller oven). At the university, the specimens were fired in a Termolab oven and the firing cycle was: i) heating rate of 5 ºC/min until 980 ºC; ii) dwell of 15 min and iii) cooling rate of 15 ºC/min. At industrial scale the maximum temperature achieved was 1000 ºC. These temperatures were measured with Buller Rings (from Mantec refractories, reference TR27/84).

Characterization techniques

Physicochemical characteristics of calcium carbonate powders

The chemical composition of the limestone and eggshell was evaluated by X-ray fluorescence (XRF) in a Philips X'Pert PRO MPD spectrometer. X-ray diffraction (XRD) analyses were performed at room

temperature in a PANalytical XPert PRO diffractometer (Ni-filtered CuKa radiation, PIXcel 1D detector) and the exposition corresponded to about 2 seconds per step of 0.02º 2θ at room temperature. Differential thermal and thermogravimetric analyses (DTA/TG) of the limestone and eggshell were performed in a Hitachi equipment (model STA300), from room temperature until 1200 °C, with a heating rate of 10 °C/min. The particle size distribution of the mixtures (limestone/eggshell and kaolin) was determined by the laser diffraction method in a Coulter LS230 analyzer (Fraunhofer optical model), and two analyses were performed for each sample. Finally, the eggshell waste (inner and outer shell) and calcium carbonate powders (limestone and eggshell) were carbon-coated and the microstructures were observed in a scanning electron microscope (SEM) Hitachi SU-70, 15kV acceleration voltage.

Pastes and Specimens Characterization

X-ray diffraction (XRD) analyses of the different pastes were also determined using the same conditions as in the calcium carbonate powders. DTA/TG were performed in three produced pastes (L100D4, L50E50D4 and E100D4) and the maximum temperature used was 1000ºC with a heating rate of 10 °C/min. Dilatometric analyses of the developed pastes were accessed in a dilatometer (TERMOLAB 412/17) to determine the linear thermal expansion coefficient (ISO 10545-8 [2]).

The specimens' characterization was carried out and 10 replicates were used in each test. The weight loss and total firing shrinkage were calculated taking into account the weight and length, respectively, of the dried and fired specimen. The flexural strength of the dried and fired specimens was evaluated in a universal testing machine (Shimadzu Autograph AG-25TA) with a load cell of 20 MPa according to ISO 10545-4 [3]. The distance between supports was 100 mm and a displacement rate of 5 mm/min was used. The apparent density and water absorption (according to ISO 10545-3 [4]) of the fired specimens were determined. SEM analysis of the polished sintered samples (L100D4, 50L50ED4, 100ED4, 100ED5.5) was also performed. Finally, to evaluate the color of the fired specimens CIEL*a*b* method was used and the color coordinates (L^*, a^* and b^*) were measured with a portable CHROMA METER CR-400 colorimeter (KONICA MINOLTA). The colorimetric stability, ΔE, was calculated according to the following equation [5]:

$$\Delta E = \sqrt{(L_A^* - L_B^*)^2 + (a_A^* - a_B^*)^2 + (b_A^* - b_B^*)^2}$$ Equation 1

where A and B represent the color coordinates of two specimens.

4.1.1. Results obtained

Calcium carbonate powders characterization

The results obtained by X-ray fluorescence analyses of the limestone and eggshell are presented in Table 9. As expected, both materials are mainly composed of calcium, 96.5 and 98.4 wt.%, limestone and eggshell, respectively. Moreover, the amount of other components, such as silica, alumina, etc., are smaller in the eggshell sample (1.6 wt.% *versus* 3.5 wt.% for the limestone).

Table 9 - X-ray fluorescence results of limestone and eggshell.

Components (wt.%)	Limestone	Eggshell
CaO	**96.5**	**98.4**
SiO_2	2.4	0.4
Al_2O_3	0.4	0.1
K_2O	-	0.1
MgO	0.6	1.0
Fe_2O_3	0.1	-

The diffractograms of limestone and eggshell are shown in Figure 10. It can be observed that the diffractogram of eggshells is very similar to that of the limestone presenting only one crystalline phase - calcite.
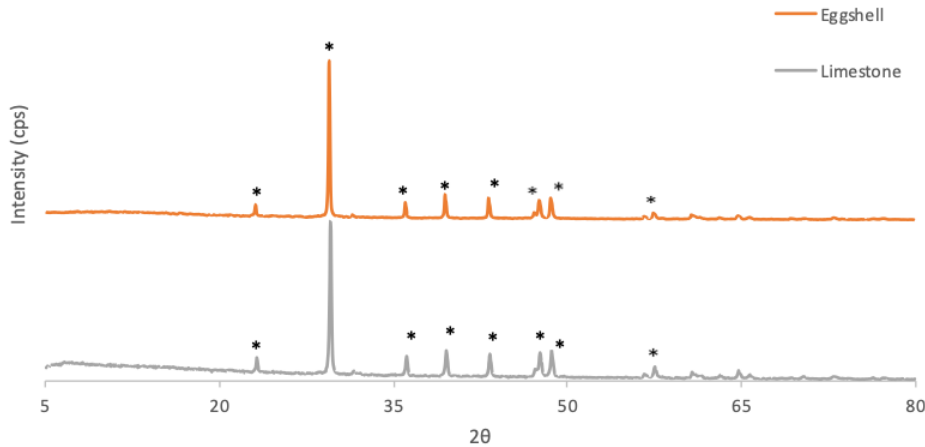

Figure 10 - XRD of limestone and eggshell where (*) represents the calcite.

The weight loss and heat flow curves of the limestone and eggshell from the DTA/TG analysis are presented in Figure 11. In the limestone, the weight loss (TG line) is accompanied by only one endothermic peak in DTA between 700 and 850 ºC, which corresponds to the calcium carbonate decomposition ($CaCO_3$ CaO + CO_2) [6]. Moreover, the sample weight seems to stabilize at around 850 °C, reaching a weight loss value of 44 wt.%. The value of the reference sample is very similar (43.6 wt.%) being due to the calcium carbonate decomposition [6]. Regarding the eggshell waste, an exothermic peak between 400-500 °C is observed accompanied by a small weight loss which corresponds to the oxidation of the organic matter [7]. These results indicate that fragments of the egg membrane remain in the powder corresponding to a weight loss below 5 wt.% which can be associated with the burning of the remaining organic membrane stuck to the shell particles. Similar to the limestone, between 650 and 800 ºC an endothermic peak ($CaCO_3$ decomposition) is observed. The weight loss stabilizes after 800 ºC being the maximum value of 48 wt.%, higher than that of the limestone. These results might indicate that the presence of eggshell waste in the formulations can negatively affect the properties of the ceramic wall tiles, namely shrinkage and water absorption.
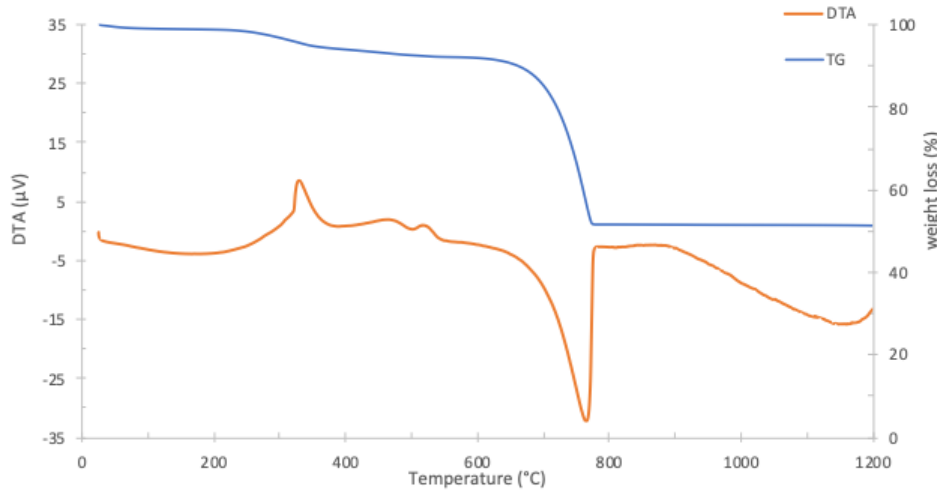
    a. Limestone
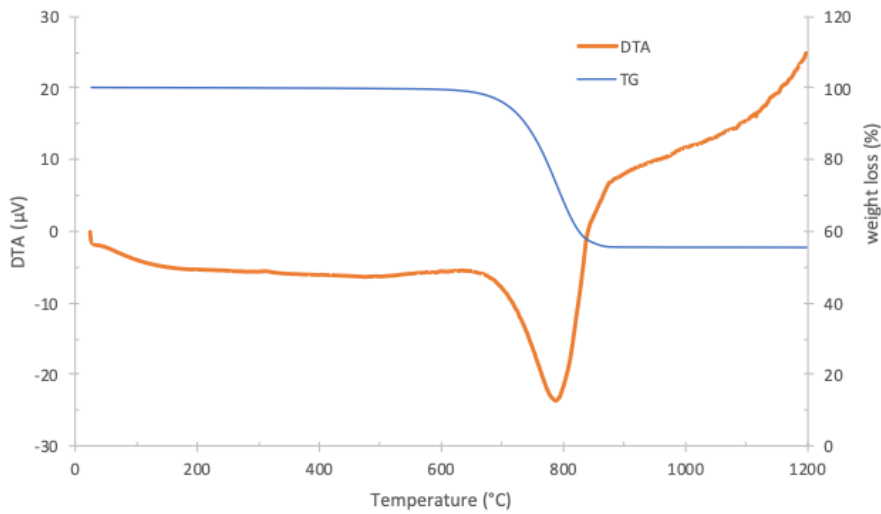
b. Eggshell

Figure 11 – DTA and TG results of: a) Limestone and b) eggshell.

The particle size distribution of eggshell mixture with different milling times (30, 60 and 90 minutes) is presented in Figure 12. As expected, the increase of the milling time leads to lower particle sizes, which is mainly observed in the cumulative volume curves (dashed curves) and in the range of the particle's diameter, differential volume curves (line curves). Table 10 presents the influence of the milling time on the D50 value for eggshell waste and limestone (92 wt.% of calcium carbonate source and 8 wt.% of kaolin). In both cases, as expected, as higher is the milling time lower is the particle size of the milled material. Moreover, to achieve a D50 of 4 μm (the reference value), a longer time is required for the eggshell waste (60 minutes) than for limestone (10 minutes). In the grinding process in a ball mill the amount of energy required depends on the initial and final particle size of the material to be ground [8]. The larger the initial particle size of the material, the more energy is required. Eggshell waste has a much coarser particle size than limestone which explains the longer grinding time to obtain a similar D50.

Table 10- Calcium carbonate mixture particle size (D50) and milling time required.

CaCO$_3$ Source	Eggshell			Limestone	
D50 (μm)	2.5	4	5.5	3.5	4

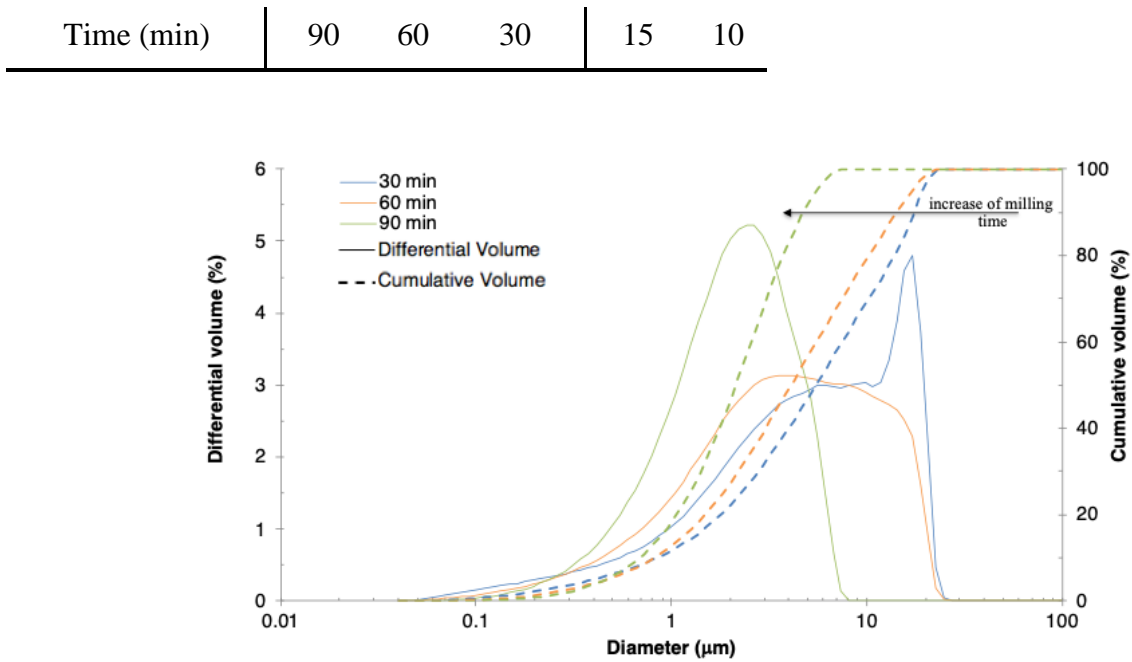| Time (min)	90	60	30	15	10

Figure 12 - Particle size distribution of eggshell mixture with different milling times: 30, 60 and 90 minutes.

Finally, SEM micrographs of the eggshell and the powders are shown in Figure 13. Figure 13A and Figure 13B, present the interior and exterior parts of the eggshell, respectively. The milled eggshell and limestone powders (D50 = 4 μm) are present in Figure 13C and Figure 13D, respectively. Figure 13A clearly shows the membrane and the shell. The eggshell structure presents a branched system made of small needles while the membrane seems to have a compact structure. Further, looking also at Figure 13B, it can be noticed that the eggshell presents different structures having thinner needles in the outer than in the inner section. In Figure 13C and Figure 13D it is possible to observe that the limestone powder presents bigger particles than the eggshell powder therefore, its size range is larger. However, in both cases, particles have several shapes and no agglomeration is observed.
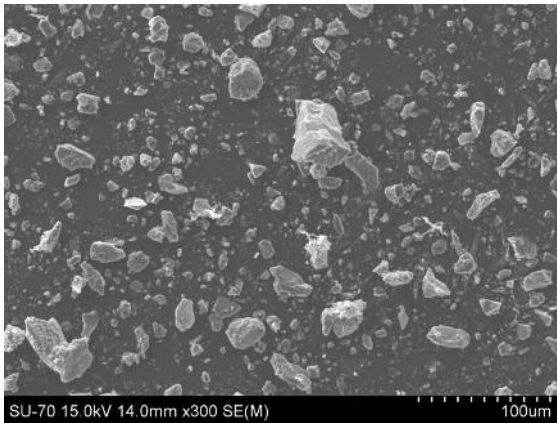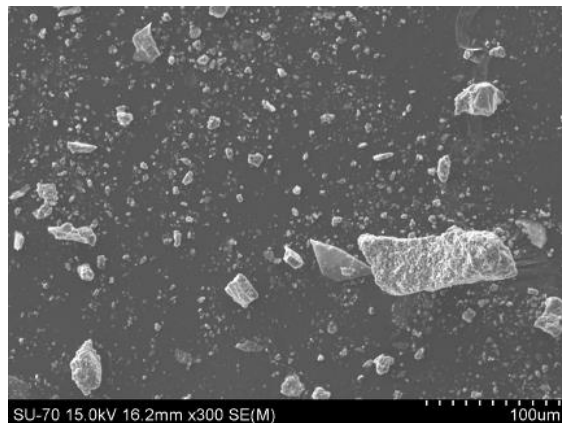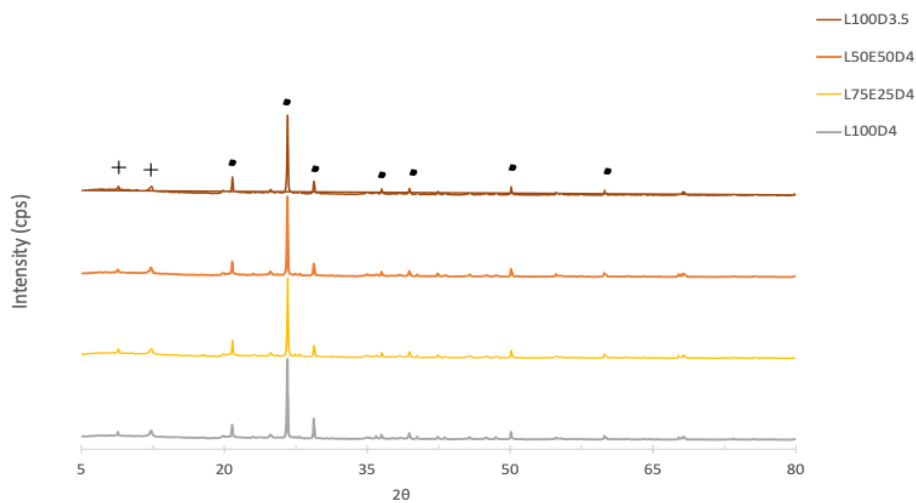
A
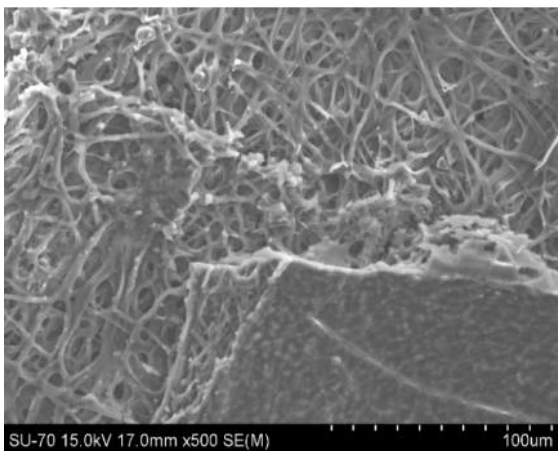
B
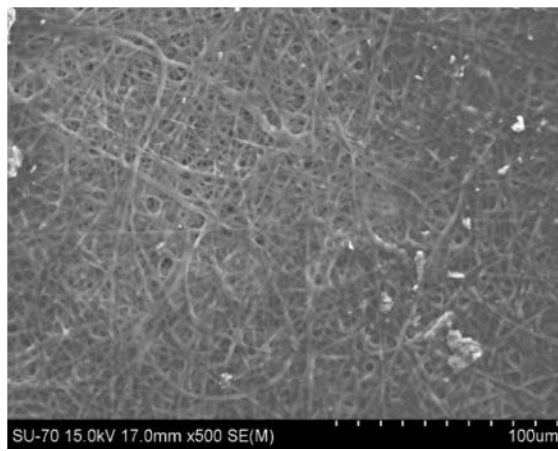
C

D

Figure 13 - SEM micrographs of: A - inner eggshell, B - outer eggshell, C - eggshell powder, D - limestone powder.

Pastes characterization

The diffractograms of the prepared pastes are present in Figure 14. The main crystalline phase, for all the compositions, is the calcite. The muscovite phase is also observed due to the presence of kaolin in the pastes [9].
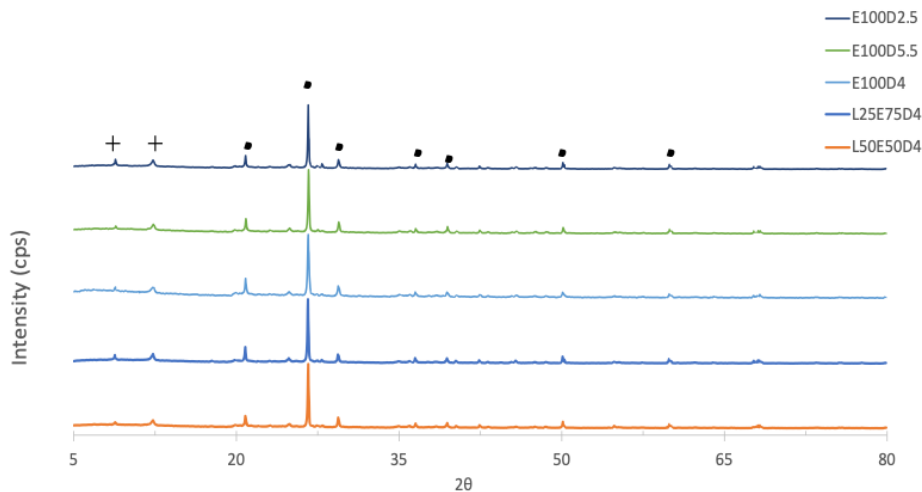
a)

b)

Figure 14 - XRD of pastes mostly with: a) limestone and b) eggshell; where (.) indicates the calcite and (+) muscovite phase.

The differential thermal and thermogravimetric analyses of the pastes with 100 wt.% of limestone (L100D4), 50 and 100 wt.% of eggshells (L50E50D4 and E100D5.5) can be observed in Figure 15. In the weight loss no differences between the pastes are noticed and, in all pastes, the weight stabilized at around 800ºC with a total weight loss of 11.3 wt.%. In the DTA, the pastes behaviour is also very similar. The first exothermic peak 100-300ºC is associated with the water release and oxidation of the organic matter. The second exothermic peak at 480-580ºC is the de-hydroxylation of clay phyllosilicates (release of the structural OH groups) being responsible for a weight loss of 3.4 wt.% [7]. Between 720ºC and 780ºC, an endothermic peak is observed, together with some weight loss, corresponding to the $CaCO_3$ decomposition.
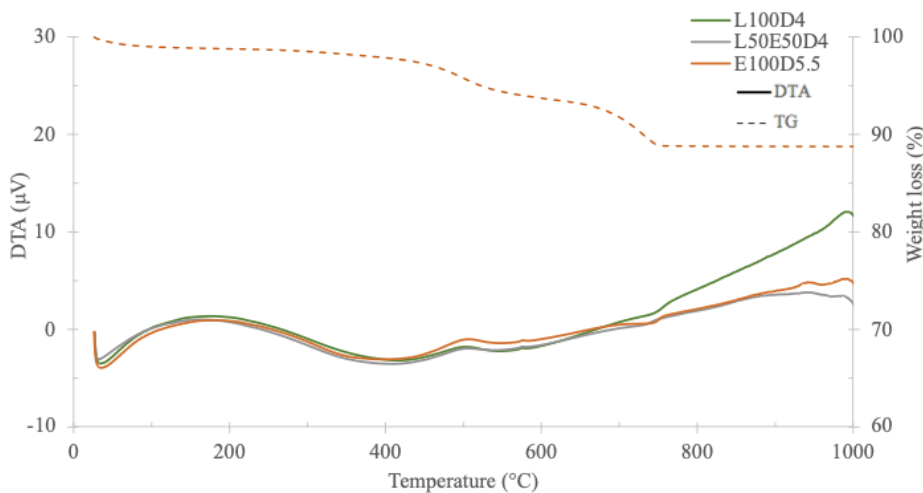

Figure 15 - Differential thermal and thermogravimetric analyses of pastes: L100D4, L50E50D4 and E100D5.5.

The linear thermal expansion coefficients (α) of the prepared formulations are presented in Table 11. All the prepared formulations exhibit very similar values (between 2.31 and 2.33 x10^{-6} 1/ºK) in the temperature range of 200-300ºC. So, the addition of eggshell waste does not affect the α value.

Table 11 - Linear thermal expansion coefficients between 200 and 300°C.

Specimens	L100D4	L75E25D4	L50E50D4	L25E75D4	E100D4	E100D5.5	E100D2.5	L100D3.5
α	2.31	2.33	2.32	2.33	2.32	2.32	2.32	2.32

(x10^{-6} 1/°K)								

Specimens' characterization

The weight loss values of the fired specimens are shown in Figure 16. All values are between 27 and 29 wt.% therefore, no significant differences are observed neither with the limestone substitution by eggshell waste nor with the particle size nor the firing conditions.
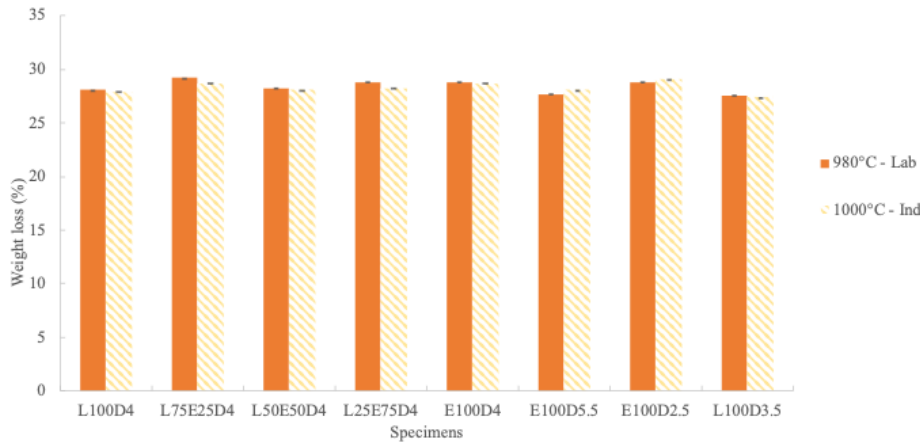

Figure 16- Weight loss of the fired specimens at different conditions: Lab - laboratory and Ind - industry.

The values of drying and firing shrinkage are shown in Figure 17. The drying shrinkage is related to the conformation method used, in this case the extrusion, being the obtained values between 3.7 and 4.7 %. The firing shrinkage presents values very low, below 0.5 %. Therefore, the calcium carbonate source (limestone or eggshell), its granulometric distribution and the used firing conditions did not affect the firing shrinkage of the specimens.
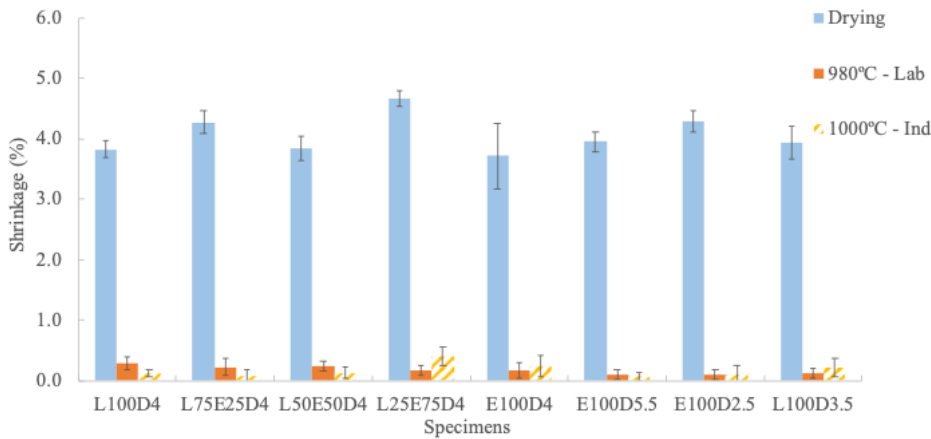

Figure 17 – Drying and firing shrinkage of the fired specimens (Lab - laboratory and Ind – industry).

The flexural strength was evaluated for the dried and fired specimens, see Figure 18. The dried specimens exhibit flexural strength values slightly lower than 4 MPa and, as in the previous results, no influence of calcium carbonate source or its particle size is observed. Looking at the flexural strength of the fired specimens, overall, its value is equal or higher for the specimens fired in the industrial furnace. This typology of material should present a mechanical strength greater than 15 MPa [10], a requirement that is met by all the compositions prepared in this work. Moreover, as expected, reducing the limestone D50 value the flexural strength of the specimens increases, e.g. 21 to 25 MPa for L100D4 and L100D3.5, respectively. Furthermore, the specimens prepared with 100 wt.% of eggshell waste (E100D4), fired at the industrial

furnace, presents a 19 % higher flexural strength than the ones prepared with limestone with the same D50 (L100D4), 25 versus 21 MPa, respectively. The flexural strength of the samples E100D4 and L100D3.5 is identical ($\approx$ 25 MPa), which suggests that bio-calcite is more reactive than limestone. This can explain the increase of the flexural strength when the same granulometry, for limestone and bio-calcite, was used. The fact that, unlike the eggshell waste, the limestone has some silica (2.4 wt.%), which is probably in the form of quartz, may also contribute to the observed behaviour.

Moreover, at the industrial furnace, it can also be observed that the specimens with 100 wt.% eggshell waste and with a higher D50 (E100D5.5) exhibits a higher flexural strength (24 MPa) than the reference (L100D4). These results suggest that, for the eggshell waste, higher particles diameter (until 5.5 μm) do not affect the flexural strength of the specimens and, therefore, shorter milling times can be used reducing the associated electric costs.
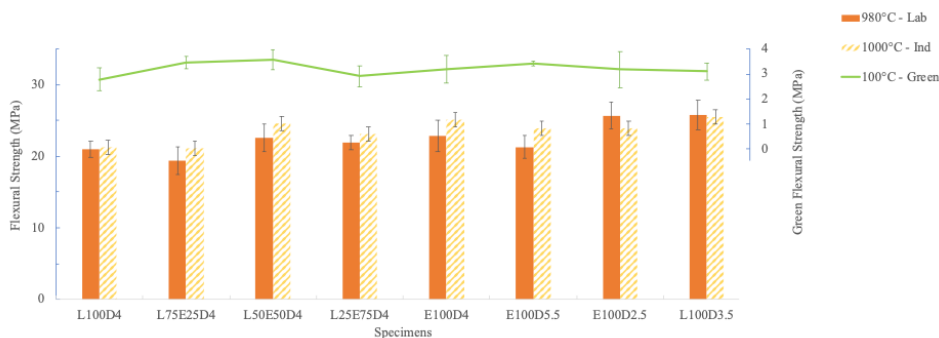

Figure 18 - Flexural strength of the dried and fired specimens at different conditions: Lab - laboratory and Ind - industry.

The values of water absorption (WA%) and geometric density of the fired specimens are presented in Table 12. For all the firing temperatures, the utilization of eggshell waste promotes a small increase in the water absorption values. Moreover, in most cases, a smaller particle size, in both limestone and eggshell, promotes higher water absorption values as well. Nevertheless, all WA% values are within the required industrial ones, according to the European Standard EN 14411 (10-20 %) [11]. Regarding the density of the specimens, no influence of the eggshell content was observed. Therefore, the specimens prepared with bio-CaCO$_3$ present a slightly higher open porosity but, looking at the flexural strength and density values, the dense phase of these specimens is more compact or have more resistants' phases than the specimens that use limestone as a calcium carbonate source.

Table 12 - Influence of waste amount, particle size and firing conditions on water absorption and geometric density of the specimens.

		L100D4	L75E25D4	L50E50D4	L25E75D4	E100D4	E100D5.5	E100D2.5	L100D3.5
980ºC	%WA	15.1±0.2	16.8±0.4	16.6±0.2	16.8±0.2	17.9±0.3	18.4±0.5	17.8±0.3	16.6±0.4
(Lab)	ρ (g/cm^3)	1.6±0.1	1.6±0.1	1.6±0.1	1.7±0.1	1.6±0.1	1.6±0.1	1.6±0.1	1.6±0.1
1000ºC	%WA	16.0±0.1	16.5±0.2	16.7±0.1	17.2±0.2	17.5±0.2	16.9±0.1	17.8±0.2	16.2±0.2
(Ind)	ρ (g/cm^3)	1.6±0.1	1.66±0.09	1.55±0.04	1.58±0.05	1.58±0.09	1.6±0.1	1.56±0.07	1.60±0.05

The SEM micrographs of the samples: L100D4, L50E50D4, E100D4, E100D5.5 are presented in Figure 19. The microstructures show that the porosity is uniformly distributed in the specimens and that, as expected, the sample prepared with the higher waste particle size (D50 = 5.5 μm) presents bigger pores.
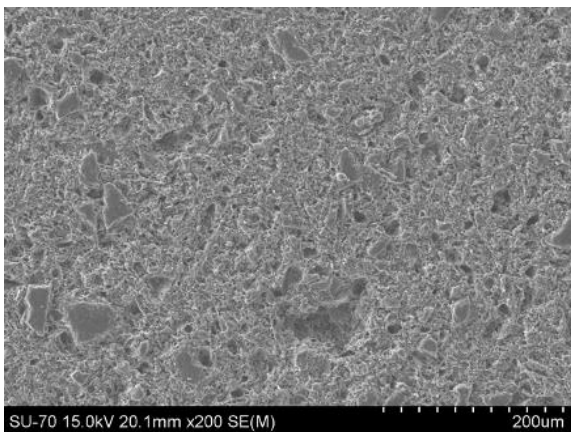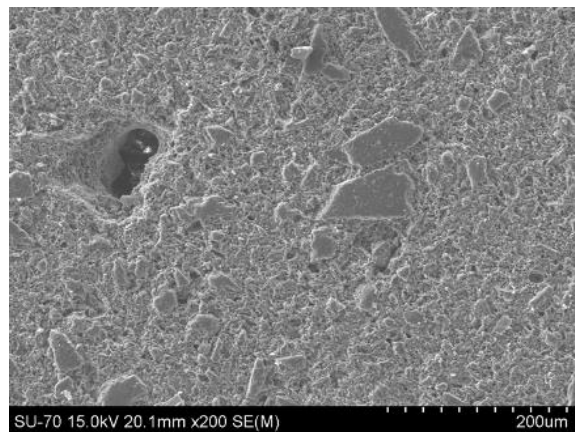
L100D4
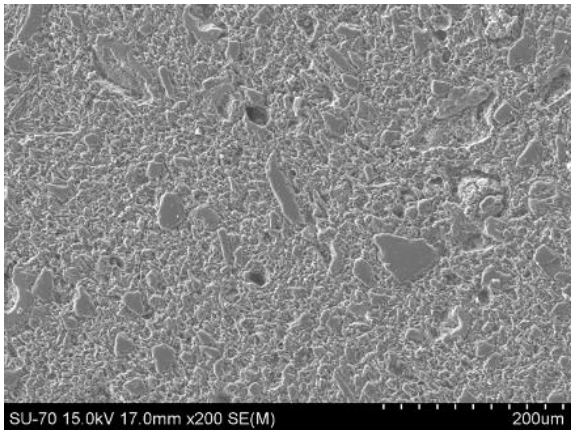
L50E50D4
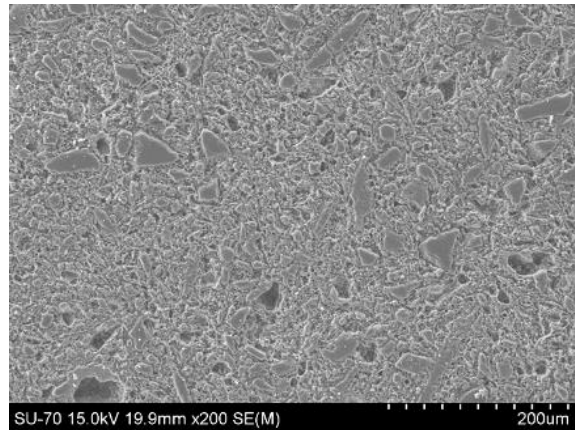
E100D4

E100D5.5

Figure 19 – SEM micrographs of fired specimens: L100D4, L50E50D4, E100D4 and E100D5.5.

The calorimetric coordinates (L^*, a^*, b^*) of all the fired specimens are shown in Table 13, together with the calculated colour difference (ΔE) relatively to the reference specimen (L100D4). It can be observed that the waste content and granulometry does not result in colour changes. The only remarkable difference ($\Delta E = 2.6$ and 3.1, Lab and Ind, respectively) is noticed for the specimen with 100 % of limestone with the smaller particle size (3.5 μm).

Table 13 – Colorimetric coordinates (L*, a*, b*) and colour difference (ΔE) of the samples. (Lab) - laboratory and (Ind) - industry.

Temperature		L100D4	L75E25D4	L50E50D4	L25E75D4	E100D4	E100D5.5	E100D2.5	L100D3.5
980ºC (Lab)	L*	82.5±0.1	82.4±0.2	82.3±0.1	83.3±0.2	82.9±0.1	83.0±0.2	82.4±0.1	81.8±0.1
	a*	5.9±0.1	6.2±0.1	6.2±0.2	5.7±0.0	6.5±0.1	6.1±0.1	6.8±0.1	7.1±0.1
	b*	18.7±0.3	19.7±0.4	20.2±0.4	18.3±0.2	19.7±0.1	19.0±0.1	19.8±0.3	21.0±0.2
	ΔE		1.5	0.9	1.0	1.3	1.4	0.7	2.6
Colour									
1000ºC (Ind)	L*	83.0±0.5	83.6±0.1	83.2±0.4	83.6±0.3	83.7±0.2	84.3±0.3	83.6±0.3	82.8±0.3
	a*	4.4±0.1	4.2±0.1	4.5±0.1	4.1±0.0	4.5±0.1	4.1±0.1	4.7±0.0	4.9±0.1
	b*	15.8±0.2	16.0±0.3	16.7±0.5	15.2±0.7	16.1±0.4	15.0±0.5	15.7±0.2	16.4±0.4
	ΔE		1.1	0.8	0.9	1.4	1.2	0.9	3.1
Colour									

References

1. Cuff YH (1996) Ceramic Technology for Potters and Sculptors. University of Pennsylvania Press

2. Organization for Standardization I (2014) ISO 10545-8:2014 Ceramic tiles — Part 8: Determination of linear thermal expansion

3. Organization for Standardization I (2019) ISO 10545-4:2019 Ceramic tiles — Part 4: Determination of modulus of rupture and breaking strength

4. Organization for Standardization I (2018) ISO 10545-3:2018 Ceramic tiles — PART 3: Determination of water absorption, apparent porosity, apparent relative density and bulk density

5. Mokrzycki WS, Tatol M (2011) Colour difference Delta-E. A survey. Machine Graphics and Vision 20:383–411

6. Földvári M (2013) Handbook of the thermogravimetric system of minerals and its use in geological practice. Central European Geology 56:. https://doi.org/10.1556/ceugeol.56.2013.4.6

7. Galán-Arboledas RJ, Álvarez de Diego J, Dondi M, Bueno S (2017) Energy, environmental and technical assessment for the incorporation of EAF stainless steel slag in ceramic building materials. J Clean Prod 142:. https://doi.org/10.1016/j.jclepro.2016.11.110

8. Richardson JF, Harker JH, Backhurst JR (1991) Coulson and Richardson's Chemical Engineering Volume 2: Particle Technology and Separation Processes. Chem Eng Sci 2:

9. Valášková M, Klika Z, Novosad B, Smetana B (2019) Crystallization and quantification of crystalline and non-crystalline phases in kaolin-based cordierites. Materials 12:. https://doi.org/10.3390/ma12193104

10. SACMI (2006) Applied ceramic technology

11. European Committee for Standardization C (2016) EN 14411 - Ceramic tiles - Definition, classification, characteristics, assessment and verification of constancy of performance and marking